Scaling Immiscible Flow in Porous Media

Summary: Centrifuge modelling is a technique that has proved useful in the study of miscible transport processes through porous media. This report presents a discussion on the feasibility of modelling immiscible flow processes using a geotechnical centrifuge, with particular reference to the phenomena of fingering and residual entrapment.

The analysis of scaling for the mechanism of fingering indicates that unstable wetting displacements can be modelled using centrifuge testing techniques. However, scaling analyses for the mechanism of capillary entrapment show that above certain critical Capillary and Bond numbers, the degree of non-aqueous phase liquid entrapment will be lower in a centrifuge model that the corresponding prototype. Nonetheless, it is argued this does not prohibit centrifuge modelling from making a useful contribution towards the study of immiscible flow processes in porous media.

1. Introduction

In addition to miscible fluids, hazardous wastes are also frequently found in the form of nonaqueous phase liquids (NAPLs), which are sparing soluble in water. Recently, there has been much interest in predicting how these chemicals behave in both unsaturated and saturated zones of aquifer.

Immiscible displacements are characterised by viscosity and density differences between the fluids involved, and by surface tension forces (Kueper and Frind, 1988). In addition, the influence of both porous media heterogeneity and fluid wetting properties are of utmost importance.

This report addresses the potential for centrifuge modelling of immiscible flow in porous media, with particular reference to the processes of (i) unstable, wetting displacements and (ii) stable, non-wetting displacements.

2. General Scaling Relationships

General scaling relationships for flow phenomena in the centrifuge have been developed by numerous research workers (see for example Goodings, 1984 and Arulanadan et al., 1988). For a reduced scale centrifuge model test conducted using prototype soil and fluids, the relationships given in Table 1 are either evident or well established. Thus, in what follows, it will be assumed that these relationships are also applicable to the centrifuge modelling of immiscible flow processes.

3. Scaling of Unstable Wetting Displacements

The potential for centrifuge modelling of stable wetting displacements has been investigated by Illangasekare et al. (1991), who demonstrated the feasibility of modelling the stable (one-dimensional) infiltration of a light non-aqueous phase liquid (LNAPL) into both dry and residually saturated soil.

As an alternative to stable displacements, wetting fronts infiltrating the unsaturated zone can, under certain conditions, become unstable and break into fingers, which move vertically to the water table, bypassing a large proportion of the vadose zone (Glass et al., 1991). Immiscible transport under these circumstances is extremely non-uniform. As a result, contaminant loading at the water table will be quite different than if transport is assumed to be one-dimensional.

The subject of wetting front instability has received increased attention recently, with an emphasis on the formulation of stability criteria and relationships for finger properties as a function of system parameters. This section develops scaling laws for the centrifuge modelling of 'wetting front instability' and discusses whether the centrifuge would be a useful tool with which to study this problem.

The important factors used to characterise unstable wetting displacements are (i) the conditions for the onset of fingering, (ii) the finger width and (iii) the finger velocity.

Conditions for the onset of 'wetting front instability' are generally derived from linear analyses, that consider the stability of a small perturbation at the macroscopic interface separating the two immiscible fluids (see for example Kueper and Frind, 1988). It can be shown that the conditions for unstable flow depend upon the density and viscosity contrast between the two fluids, the base flow rate and the curvature of the initial perturbation.

For two-dimensional disturbances, the onset of fingering is associated with a perturbation containing wavelengths (tip to tip separations) greater than a critical wavelength λ_c.

By extending the work of Hill (1952), Chouke et al. (1959) derived the following expression for λ_c;

$$\lambda_c = 2\pi\left[\frac{\sigma^* k_f}{u\theta_f(\mu_2-\mu_1) + k_f g(\rho_1-\rho_2)}\right]^{\frac{1}{2}} \qquad (1)$$

where σ^* is the 'effective macroscopic surface tension', k_f is the

effective permeability of the infiltrating fluid at the front, u is the velocity of an unperturbed flat front, θ_f is the volumetric fluid content at the front, μ is fluid viscosity, ρ is fluid density and subscripts 1 and 2 refer to the infiltrating (wetting) and displaced (non-wetting) fluids, respectively.

In their derivation of λ_c, Chouke et al. (1959) assumed the following relationship between macroscopic frontal curvature and a pressure jump across the front:

$$p_1 - p_2 = \sigma * \left[\frac{1}{r_1} + \frac{1}{r_2} \right] \qquad (2)$$

where p denotes pressure and r_1 and r_2 are the two principle radii of curvature for the macroscopic front.

While the relationship given by Equation 2 will apply to Hele-Shaw cells and within the pores of a porous medium, its validity at a macroscopic level in a porous media has been questioned by Homsy (1987) and Glass et. al (1991).

Homsy (1987) suggests that observed estimates of the macroscopic curvature at a front compare well with those given by Equation 2, if the empirical 'effective macroscopic surface tension' is defined as

$$\sigma * = \frac{\sigma L}{k^{0.5}} \qquad (3)$$

where L is a macroscopic, horizontal dimension of the problem, k is the permeability of the medium and σ is the molecular surface tension.

As an alternative, Glass et al. (1991) propose the following expression for λ_c

$$\lambda_c = \frac{2\pi\Gamma(\mu_1+\mu_2)\theta_f}{u\theta_f(\mu_2 - \mu_1)+k_f g(\rho_1-\rho_2)} \qquad (4)$$

where Γ is defined by

$$\Gamma = \int_{\psi_0}^{\psi_f} \frac{K d\psi}{\theta_F - \theta_0} \qquad (5)$$

where K is the hydraulic conductivity, ψ is the pressure head of the infiltrating fluid, and the subscripts 0 and F denote values at the front and back of a capillary-induced 'diffusion zone' at the infiltrating front, respectively.

The average finger width or diameter is usually obtained through linear stability analysis by finding the most rapidly growing wavelength. However, it is worth noting that linear stability analysis is only valid for infinitesimal disturbances. Therefore, there is no guarantee that the wavelengths which initially grow the most rapidly will end up giving the dominant finger width, especially in a highly non-linear system (Glass et al., 1989).

Using dimensional analysis applied at the finger scale, Glass et al. (1989) derived the following approximation for finger width, w;

$$w = \frac{S_F^2}{K_F(\theta_F - \theta_0)} f_{dF}(R_F) \qquad (6)$$

where f_{dF} is a function of R_F, the dimensionless flux-conductivity ratio ($R_F = q_F/K_F$) and S is the sorptivity, which parameterizes the movement of wetting fluid due to capillary action in the absence of gravity. The approximate formula of Parlange (1975) gives S_F as

$$S_F^2 = \int_{\theta_0}^{\theta_F} (\theta + \theta_F - 2\theta_0) D \, d\theta \qquad (7)$$

where D is the diffusivity, which, like conductivity, varies non-linearly with θ.

Glass et al. (1989) use the linear stability analysis of Parlange and Hill (1976) to show that $f_{dF}(R_F)$ is initially equivalent to $\pi/(1-R_F)$ for a two-dimensional system.

The finger velocity, u_f, will depend upon the same system parameters as finger width. Again, using dimensional analysis applied at the finger scale, Glass et al. (1989) derive the following expression for u_f;

$$u_f = \frac{K_F}{\theta_F - \theta_0} f_{vF}(R_F) \qquad (8)$$

where f_{vF} is also a function of R_F.

3.1 Scaling Ratios

Equations 1 - 8 can be used to derive scaling ratios relevant to the centrifuge modelling of unstable wetting displacements.

For similitude between model and prototype with respect to the conditions for the onset of fingering, the critical wavelength, λ_c should be N times higher in the prototype than the centrifuge model; in other words, $\lambda_{c(r)} \equiv N$, where r denotes the ratio between a value in the prototype to that in

the model. This criterion ensures that the initial wavelength (tip to tip separation) of disturbances observed during the onset of fingering is N times smaller in a centrifuge model than the corresponding prototype.

In the preceding Section, definitions of λ_c were presented by either Equation 1, in conjunction with Equation 3, or by Equations 4 and 5.

Using the definition given by Equation 1, we may state that

$$\lambda_{c(r)} \equiv \left[\frac{\sigma^*_r k_{f(r)}}{u_r \theta_{f(r)} (\mu_{2(r)} - \mu_{1(r)}) + k_{f(r)} g_r (\rho_{1(r)} - \rho_{2(r)})} \right]^{\frac{1}{2}} \qquad (9)$$

From Table 1, $g_r = u_r = 1/N$ and $\mu_r = \rho_r = 1$.

Experimental evidence indicates that θ_f is approximately equal to θ_s, the saturated value of the infiltrating fluid content (Glass et. al., 1989). Thus, it is reasonable to assume that $\theta_{f(r)} = 1$, which, in turn, suggests that $k_{f(r)} = 1$.

From Equation 3,

$$\sigma^*_r \equiv \frac{\sigma_r L_r}{k_r} = N \qquad (10)$$

Substitution of the above ratios into Equation 9 leads to the conclusion that

$$\lambda_{c(r)} \equiv \left[\frac{N}{1/N} \right]^{\frac{1}{2}} = N \qquad (11)$$

Alternatively, we can use the definition of λ_c given by Equation 4 to state that

$$\lambda_{c(r)} = \frac{\Gamma_r (\mu_{1(r)} + \mu_{2(r)}) \theta_{f(r)}}{u_r \theta_{f(r)} (\mu_{2(r)} - \mu_{1(r)}) + k_{f(r)} g_r (\rho_{1(r)} - \rho_{2(r)})} \qquad (12)$$

where, from Equation 5,

$$\Gamma_r \equiv K_r \psi_r = 1 \qquad (13)$$

Note, that the value of θ_0 describes the initial volumetric content of the infiltrating fluid present in the medium before the start of infiltration. If 'pre-wetting' of the medium by the infiltrating fluid has not occurred,

$\theta_0 = 0$. Otherwise, θ_0 will be determined by the past history of the soil mass. Thus, to obtain the correct initial conditions in a reduced scale centrifuge model (i.e., to ensure that $\theta_{0(r)} = 1$), it is necessary that the model preparation procedure fully accounts for the wetting history of the prototype under investigation.

Substitution of all relevant ratios into Equation 12 leads us to conclude that

$$\lambda_{c(r)} \equiv \frac{1}{1/N} = N \tag{14}$$

Both Equations 11 and 14 satisfy the criteria for similitude between model and prototype with respect to the conditions for the onset of fingering.

For the correct scaling of average finger width between model and prototype, it is also necessary that $w_r = N$. In other words, that the width of fingers formed in a centrifuge model are N times smaller than those formed in the prototype.

Using the approximation for finger width given by Equation 6, we may state that

$$w_r \equiv \frac{S^2_{F(r)}}{(\theta_{F(r)} - \theta_{0(r)})K_{F(r)}} R_{F(r)} \tag{15}$$

where, from Equation 7,

$$S^2_{F(r)} \equiv \theta_r D_r = 1 \tag{16}$$

and where

$$R_{F(r)} \equiv \frac{q_{F(r)}}{K_{F(r)}} = 1 \tag{17}$$

By substituting all applicable ratios into Equation 15, we find that

$$w_r \equiv \frac{1}{1/N} = N \tag{18}$$

Thus, the correct scaling of finger width may be achieved during reduced scale centrifuge modelling.

Finally, to ensure similitude, the scaling laws derived for flow phenomena require that flow velocities in a centrifuge model be N times higher than those in the corresponding prototype. Thus, it is necessary that the finger

velocity u scales as $u_{f(r)} = 1/N$.

The finger propagation velocity was given by Equation 8. This equation can be used to state that

$$u_{f(r)} \equiv \frac{K_{F(r)}}{\theta_{F(r)} - \theta_{0(r)}} R_{F(r)} \qquad (19)$$

Provided that centrifuge model preparation procedure has fully accounted for the wetting history of the prototype, $\theta_{0(r)} = 1$.

Substitution of the relevant ratios into Equation 19 leads to the conclusion that

$$u_{f(r)} = \frac{1}{N} \qquad (20)$$

Hence, the finger propagation velocity should scale in accordance with the general requirement for scaling of fluid velocity.

3.2 Discussion

The scaling ratios presented above have theoretically demonstrated the feasibility of modelling unstable wetting displacements using a geotechnical centrifuge. However, as in all cases, the applicability of these ratios will be subject to certain conditions.

It has been stated that wetting front instabilities are initiated by perturbations containing wavelengths greater than the critical wavelength λ_c. As initial perturbations at the planer interface between the infiltrating and displaced fluids are the result of microscopic heterogeneity in an otherwise macroscopically homogeneous media, it is evident that the minimum wavelength contained in a perturbation must be of the order of the grain size, d, of the material. It is also evident that the maximum wavelength contained in a perturbation must be of the order of the macroscopic horizontal dimension of the problem, L. Thus, for the initiation of wetting front instability, $d < \lambda_c < L$. As both λ_c and L scale during centrifuge modelling, while d does not, there may be some instances where conditions admit instability in the prototype but not in the centrifuge model; in other words where $\lambda_{c(m)} < d < \lambda_{c(p)}$.

The arguments presented in the preceding sections have been based on a assumption that fingering during wetting front instability is characterised by some macroscopic continuum scale (Homsy, 1987). For this assumption to be reasonable, the average finger width must extend over several pore scales in both model and prototype. Again, as the finger width scales during centrifuge modelling while the pore scale does not, there may be

some instances where the average finger width in a centrifuge model is no longer large enough in comparison with the average pore scale, to be deemed macroscopic.

Finally, for cases where the medium under consideration is not homogeneous on a macroscopic scale, the development and propagation of wetting front instabilities will be dominated by the size and location of macroscopic heterogeneities within the medium. Under these circumstances, reduced scale centrifuge modelling is not likely to duplicate the prototype behaviour.

3.3 Verification of Scaling Ratios

It is suggested that verification of the scaling ratios for wetting front instability is conducted by performing 'modelling of models' over a range of *g*-levels spanning from, say 20*g* to 100*g*. For simplicity, these experiments could, at first, consider the infiltration of a NAPL into an initially dry homogeneous material. At a later stage, infiltration into partially saturated media could also be considered.

It is advised that the tests be conducted in a rectangular chamber of soil. The length of the chamber needs to be longer than the critical wavelength calculated for the lowest *g*-level. If the thickness of the chamber is less than the minimum finger width, a two-dimensional flow field will be forced. Thus, the width of the chamber should be less than the minimum finger width at the highest *g*-level. The chamber should be as high as possible, to enable observations of finger growth over the largest possible distance.

Ideally, the experiments should be conducted using a fine grained material, such as silt. This should ensure, even at high *g*-levels, a reasonable ratio between the finger width and the average pore size of the medium. In all cases, the initial packing of the medium will be important, as uniformity of packing between experiments must be guaranteed.

Glass et al. (1991) have shown that infiltration into an initially dry, homogeneous porous medium can be unstable when the flux through the system is less than its saturated conductivity ($R_f < 1$). However, work by Glass et al. (1989) has also demonstrated that, at a constant *g*-level, finger width increases with increasing R_f. Hence, it is suggested that the experiments be carried out using an R_f as close to unity as is attainable for an unstable system, in order to guarantee a maximum finger width in all experiments.

In the first instance, direct visualisation techniques should be sufficient to demonstrate the validity of the scaling ratios.

4. Scaling of Non-Wetting Phase Capillary Trapping

When a wetting fluid, such as water, displaces a non-wetting fluid, such as a non-aqueous phase liquid, in a porous medium, a proportion of the NAPL will remain entrapped in the medium pores once the wetting front has passed. In general, the NAPL is trapped in the form of discontinuous 'blobs' or 'ganglia', whose complicated morphology is strongly influenced by the geometry of the pore space.

In a dual, liquid phase porous media system, the proportion of entrapped NAPL (often referred to, misleadingly, as the 'residual saturation' of the NAPL), is a function of the capillary pressure between the NAPL and the wetting phase. On a superficial level, it appears that the length of trapped blobs can be related to the viscous and gravity forces acting within the system (Mayer and Miller, 1994), whilst the cross-sectional area and spatial distribution of the blobs is more strongly dependent on the actual fabric of the medium itself.

Figure 1 illustrates an idealised mechanism for blob entrapment. As one fluid bank displaces another, the displacement front will include advancing fingers of the displacing phase and trailing fingers of the displaced phase. When these phases are immiscible, an isolated blob will be formed when a trailing finger become disconnected through imbibition[1] in the region marked B (Morrow, 1979). However, if imbibition first occurs in the region marked A, the trailing finger will not be lost to the continuous bank.

The supplementary pressure needed in region A to prevent entrapment is given by the difference in the imbibition pressures for regions A and B. In a moving flow system, the supplementary pressure can be provided by either viscous pressures, buoyancy pressures or a combination of the two.

The supplementary pressure provided in the direction of flow by viscous forces in the aqueous phase acting over the length of an individual blob of NAPL can be computed using Darcy's law; viz

$$\Delta p_{s(v)} = \frac{v_a \, \mu_a \, l}{k} \qquad (21)$$

where v_a is the aqueous phase Darcy velocity, μ_a is the aqueous phase viscosity and l is the length of a blob measured in the direction of v_a.

Buoyancy forces will also act on the blob if there is a difference between NAPL and aqueous phase densities. The vertically directed supplementary

---

[1] Imbibition refers to the displacement of the non-wetting phase by the wetting phase.

pressure due to buoyancy forces across the blob can be written as

$$\Delta p_{s(b)} = -g(\rho_a - \rho_n)l \tag{22}$$

where ρ_a is the density of the aqueous phase, ρ_n is the density of the NAPL and g is the gravity vector.

For vertical flow, the viscous and gravity pressure terms can be summed, yielding

$$\Delta p_s = \Delta p_{s(v)} + \Delta p_{s(b)} = \left(\frac{v_a \mu_a}{k} - g(\rho_a - \rho_n) \right) l \tag{23}$$

From Equation 23, it is apparent that the supplementary pressure provided in the direction of flow will be greatest for the upward non-wetting displacement of an LNAPL (Light Non-Aqueous Phase Liquid), or for the downward non-wetting displacement of a DNAPL (Dense Non-Aqueous Phase Liquid).

For simplicity, we will assume in what follows, that we are dealing exclusively with the upward non-wetting displacement of an LNAPL. However, the scaling arguments that succeed will be equally applicable to more general situations.

The difference in imbibition the pressures for regions A and B will be given by

$$\Delta p_{imb} = 2\sigma_{na} \left(\frac{1}{r_B} - \frac{1}{r_A} \right) \approx \frac{2\sigma_{na}}{r} \tag{24}$$

where it has been assumed that the contact angle is zero, and where the parameter r describes the ratio between a microscopic characteristic length for the porous medium and the limiting curvature for imbibition at the fluid phase interface (Melrose and Brandner, 1974).

If we equate Equation 24 with Equation 23, we can derive and expression for the maximum length of a trapped blob in the direction of aqueous phase flow; viz

$$l_{max} = \frac{2}{r} \left(\frac{v_a \mu_a}{k \sigma_{na}} + \frac{g(\rho_a - \rho_n)}{\sigma_{na}} \right)^{-1} \tag{25}$$

In problems of immiscible flow, the ratio of viscous forces to capillary forces is often described by the dimensionless capillary number

$$C_a = \frac{v_a \mu_a}{\sigma_{na}} \tag{26}$$

In addition, the ratio of buoyancy forces to capillary forces is frequently expressed by the Bond number

$$B_o = \frac{g(\rho_a - \rho_n)R^2}{\sigma_{na}} \tag{27}$$

where R is a characteristic pore size of the medium.

Substituting C_a and B_o into Equation 25 gives

$$l_{max} = \frac{2}{r}\left(\frac{C_a}{k} + \frac{B_o}{R^2}\right)^{-1} \tag{28}$$

Thus, for any given system, an increase in the value of either C_a or B_o will lead to a reduction in the average length of blobs trapped behind the wetting front.

4.1 Scaling Ratio for Maximum Blob Length

Through inspection of Equations 26 and 27, it is straightforward to show, that for centrifuge model tests conducted using prototype soil and fluids, the Capillary and Bond numbers will scale as

$$C_{a(r)} = \frac{1}{N} \quad \textit{and} \quad B_{o(r)} = \frac{1}{N} \tag{29}$$

Substitution of the above relationships into Equation 28 leads to that conclusion that

$$l_{max(r)} = N \tag{30}$$

In other words, the average maximum length of a trapped blob with be N times smaller in a centrifuge model than the prototype. Therefore, the scaling ratio for blob length is in accordance with the general scaling factor for length, suggesting that the maximum blob length will be correctly scaled during centrifuge testing.

4.2 Scaling of Entrapped NAPL Saturation

For most problems involving immiscible flow, our main interest will lie in predicting the degree of entrapped NAPL saturation following a non-wetting displacement, and not the maximum length of entrapped blobs.

As noted above, NAPL entrapment is initiated by capillary forces and overcome by either viscous pressure forces, buoyancy forces or a combination of the two. The capillary forces that bring about entrapment will be a function of the fabric of the porous medium and the interfacial tension between the NAPL and the aqueous phase fluid. Thus, the distribution of sites that may potentially trap a NAPL blob of length l should not vary between the prototype and a centrifuge model constructed using prototype material.

If we assume that there is a log-linear relationship between the length, l, of a blob that may potentially become entrapped at a site, and the cumulative number of sites that may entrap blobs of length l, we can plot the relationship given in Figure 2.

The minimum potential blob length is likely to be of the order of 0.1d, where d is the average particle diameter of the medium. Variations of blob size distributions over approximately two orders of magnitude have been reported in the literature (see for example, Chatzis et al., 1983), suggesting a maximum potential blob length of approximately 10d and a mean potential blob length of d.

Under low Capillary and Bond number conditions, the theoretical maximum length for a trapped blob will probably exceed 10d, suggesting that blobs will become entrapped at all potential sites. Thus, these conditions are likely to provoke the maximum degree of entrapped NAPL saturation, S_{max}. Work reported in the literature (Morrow and Songkran, 1981, Mayer and Miller, 1994) implies that low Capillary and Bond number conditions may operate when either number, or their effective sum, falls below approximately 10^{-3}.

As the values of C_a and B_o increase, the value of l_{max} will decrease. When l_{max} falls below the maximum potential blob length, blobs with lengths $l > l_{max}$ will no longer become entrapped. Hence, under these conditions, the degree of entrapped NAPL saturation will be given by $S = f\ S_{max}$, where $f < 1$.

We can use Figure 2 to obtain an estimate for the value of f. If we express l_{max} as a ratio of d, i.e, $l_{max} = C\ d$, where C is a 'constant' for a fixed value of C_a and B_o, then the magnitude of f can be described by

$$f = 0.5 \left(\log_{10} \frac{C}{0.1}\right) \qquad (31)$$

Problems will arise in the centrifuge modelling of non-wetting phase entrapment unless $f_r = 1$. When $f_r \neq 1$, the degree of entrapped NAPL will be

less in the centrifuge model than the prototype.

There are two conditions under which f_r will equal unity. The first condition arises when f = 0 in both model and prototype. This would imply that the Capillary and Bond numbers were sufficiently high in the prototype to ensure zero entrapment of NAPL behind the wetting front. Clearly, this situation would also be repeated in the centrifuge model of the prototype, where the Capillary and Bond numbers would be N-times higher. The second condition arises when f = 1 in both model and prototype. This would imply that the effective sum of the Capillary and Bond numbers remained below, say 10^{-3}, in both model and prototype, thereby ensuring a maximum degree of entrapped NAPL saturation in both cases. The second condition can be thought of as analogous to the condition for the correct scaling of miscible dispersion during centrifuge testing, which requires that the grain Peclet Number remains below a certain critical value in both model and prototype.

4.3 Discussion

Several assumptions have been made in the preceding sections whose validity now needs to be discussed.

The approximate formula for maximum blob length given by Equation 28 assumes a direct inverse correlation between l_{max} and C_a and B_o. Work reported in the literature suggests strong inverse correlations between l_{max} and C_a and B_o at high Capillary numbers (Mayer and Miller, 1994). However, weaker correlations have been reported between l_{max} and C_a at low Capillary numbers. This suggests that correct scaling of l_{max} may not be achieved at low Capillary numbers.

Derivations for the degree of entrapped NAPL saturation were based on an assumption that the centrifuge model was constructed using a soil representative of the prototype soil. In general, this criterion can only be met if the prototype soil is relatively homogeneous on a macroscopic scale. In addition, it is worth noting that non-wetting phase displacements often show extreme sensitivity to even relatively minor variations in soil fabric (Chatzis et al., 1983). Thus, the construction of a centrifuge model which adequately represents the prototype soil fabric may prove difficult, even for problems involving homogeneous media.

The calculations for entrapped saturation assume the solid line relationship given in Figure 3 between normalised entrapped NAPL saturation and a combined linear function of C_a and B_o. However, it is felt that the dashed line relationship given in Figure 3 probably provides a more reasonable approximation, as the form of this line agrees with relationships reported in the literature between C_a and observed NAPL

saturation (see for example, Chatzis et al., (1988).

4.4 Verification of Scaling Ratios

It is suggested that verification of the scaling ratios for non-wetting phase entrapment is conducted by performing tests over a wide range of *g*-levels spanning from, say 20*g* to 200*g*. For simplicity, these experiments could, at first, only consider the upward displacement of an LNAPL, such as Soltrol-130, by water. At a later date, more complicated problems, such as the horizontal displacement of an LNAP by water, could be considered[2].

It is advised that the initial tests be conducted in a column of uniform sand, that has initially been saturated with the LNAPL. The column should be as tall as possible to eliminate end effects (≈ 150 mm), and of sufficient diameter to eliminate edge effects (≈ 100 mm). The upward fluid velocity through the sample is probably best controlled by a displacement pump.

The effective sum of the Capillary and Bond numbers should be varied over a wide range during the test series (from, say, 10^{-4} at 20*g* to 10^{-2} at 200*g*). Tests should also be conducted at 1*g* for comparison.

Initially, the degree of entrapped LNAPL remaining after a single passage of the wetting front could be determined from subsequent weight and volumetric measurements. At a later date, experimental methods involving 'blob casting' could be used to verify whether or not maximum blob lengths scale with *g*-level.

5. Conclusions

Many hazardous waste sites and leaking underground storage tanks contain light non-aqueous phase organic liquids. Often released at or near the surface, these immiscible fluids move downward through the unsaturated zone towards the water table. Migrating as a separate phase, their behaviour changes from that of a predominately wetting displacement in the unsaturated zone, towards that of a non-wetting displacement in the saturated zone.

The feasibility of using centrifuge testing to model the stable, one-dimensional infiltration of a light non-aqueous phase liquid (LNAPL) into unsaturated soil has been demonstrated by Illangasekare et al. (1991). Scaling laws developed in this report also indicate that centrifuge testing may, in addition, be successfully used to model the unstable infiltration of an LNAPL into unsaturated soil.

---

[2] In this case, the effects of the Capillary and Bond numbers will act in directions which are transverse to each other.

Once a LNAPL reaches the saturated zone, the weight of the organic liquid depresses the capillary fringe and water table, and then redistributes laterally. The lateral distribution of the LNAPL will cause the water table to rebound, resulting in entrapment of the LNAPL in the saturated zone (Wilson et al., 1990).

Scaling laws developed for non-wetting phase entrapment suggest that the saturation of an entrapped NAPL can only be correctly modelled during centrifuge testing, if the effective sum of the Capillary and Bond numbers characterising entrapment in the model remains below a certain critical value. Otherwise, entrapped NAPL saturations are liable to be lower in a centrifuge model than the corresponding prototype.

For some classes of problem, the scale effects introduced by failing to model processes, such as non-wetting phase entrapment, are likely to be small. Under these circumstances, observations made with regard to the centrifuge model can be considered representative of the prototype behaviour. Under other circumstances, centrifuge model tests can be regarded as independent transport events, producing data under repeatable and controlled laboratory conditions. Irrespective of the validity of the scaling laws, such data may still be used (i) to test and verify existing mathematical transport codes, and (ii) to collect observations of LNAPL behaviour over a range of different conditions, including a range of Capillary and Bond numbers.

The aim of the majority of investigations into NAPL behaviour is to better understand the basic physical mechanisms controlling the movement of organic liquids in soils and groundwater. These mechanisms will be influenced by gravity driven phenomena, as well as capillary forces and viscous pressure forces. This suggests that centrifuge modelling may well be able to make a useful contribution towards this aim.

References

Arulanandan, K., Thompson, P.Y., Kutter, B.L., Meegods, N.J., Muraleetharan, K.K. and Yogachandran, C. (1988). Centrifuge modelling of transport processes for pollutants in soils, Journal of Geotechnical Engineering, ASCE, 114 (2), February 1988, pp 185-205.

Chouke, R.L., Van Meurs, P. and Van der Poel, C. (1959). The instability of slow, viscous, liquid-liquid displacements in permeable media. *Petrol. Trans. AIME*, 216: 188-194.

Chatzis, I., Morrow, R.N. and Lim, H.T. (1983). Magnitude and detailed structure of residual oil saturation, *Soc. Pet. Engs. Journ.*, April 1983, 311-326.

Chatzis, I., Kuntamukkula, M.S. and Morrow, N.R. (1988). Effect of capillary number on the microscopic structure of residual oil in strongly water-wet sandstones. *SPE Reservoir Engineering*, August 1988, 902-912.

Goodings, D.J. (1984). Relationships for modelling water effects in geotechnical centrifuge models. In: W.H. Craig (ed.) *Application of Centrifuge Modelling to Geotechnical Design*, 1-24.

Hill, S., (1952). Channelling in packed columns. *Chem. Eng. Sci.*, 1(6): 247-253.

Glass, R.J., Parlange, J.-Y. and Steenhuis, T.S. (1989). Wetting front instability, 1, Theoretical discussion and dimensional analysis, *Water Resour. Res.*, 25, 1187-1194.

Glass, R.J., Parlange, J.-Y. and Steenhuis, T.S. (1991). Immiscible displacement in porous media: Stability analysis of three-dimensional, axisymmetric disturbances with application to gravity driven wetting front instability, *Water Resour. Res.*, 27(8), 1947-1956.

Homsy, G.M. (1987). Viscous fingering in porous media. *Ann. Rev. Fluid Mech. 1987*, 19: 271-311.

Illangasekare, T.H., Znidarčić, Al-Sheridda, M. and Reible, D.D. (1991). Multiphase flow in porous media, *Centrifuge 91*, H.Y. Ko and F.G. McLean (eds.), 517-523.

Kueper, B.H. and Frind, E.O. (1988). An overview of immiscible fingering in porous media. *J. Contam. Hydrol.*, 2: 95-110.

Mayer, A.S. and Miller, C.T., (1994) The influence of porous media characteristics and measurement scale on pore-scale distributions of residual nonaqueous phase liquids, *Journ. Cont. Hydrology*, (in press).

Melrose, J.C. and Brandner, C.F. (1974). Role of capillary forces in determining microscopic displacement efficiency for oil recovery by waterflooding, *Journ. of Canadian Petroleum Technology*, 13, 54-62.

Morrow, N.R. (1979). Interplay of capillary, viscous and buoyancy forces in the mobilization of residual oil. *Journ. of Canadian Petroleum Technology*, 18(3), 35-46.

Morrow, N.R. and Songkran, B. (1981). Effect of viscous and buoyancy forces on nonwetting phase trapping in porous media, *Surface Phenomena in Enhanced Oil Recovery*, Shah, D.O. ed., Plenum Press, N.Y., 387-411.

Parlange, J.-Y., (1975). On solving the flow equation in unsaturated soils by optimization: Horizontal infiltration, *Soil Sci. Soc. Am. Proc.*, 39, 415-418.

Parlange, J. -Y. and Hill, D.E. (1976) Theoretical analysis of wetting front instability in soils, *Soil Sci.*, 122, 236-239.

Wilson, J.L., Conrad, S.H., Mason, W.R., Peplinski, W. and Hagan, E. (1990). Laboratory investigation of residual liquid organics from spills, leaks and the disposal of hazardous wastes in groundwater, *U.S. EPA Report*, EPA/600/6-90/004, April 1990.

Table 1: Centrifuge Scaling Relationships

Parameter	Prototype/model ratio
Gravity, g	1/N
Macroscopic length, L	N
Microscopic length, d	1
Pore fluid velocity, u	1/N
Seepage flux, q	1/N
Fluid pressure, p	1
Fluid pressure head, ψ	N
Time, t	N^2
Hydraulic conductivity, K	1/N
Soil permeability, k	1
Saturated fluid content, θ	1
Diffusivity	1
Fluid density, ρ	1
Fluid viscosity, μ	1

N: scaling factor

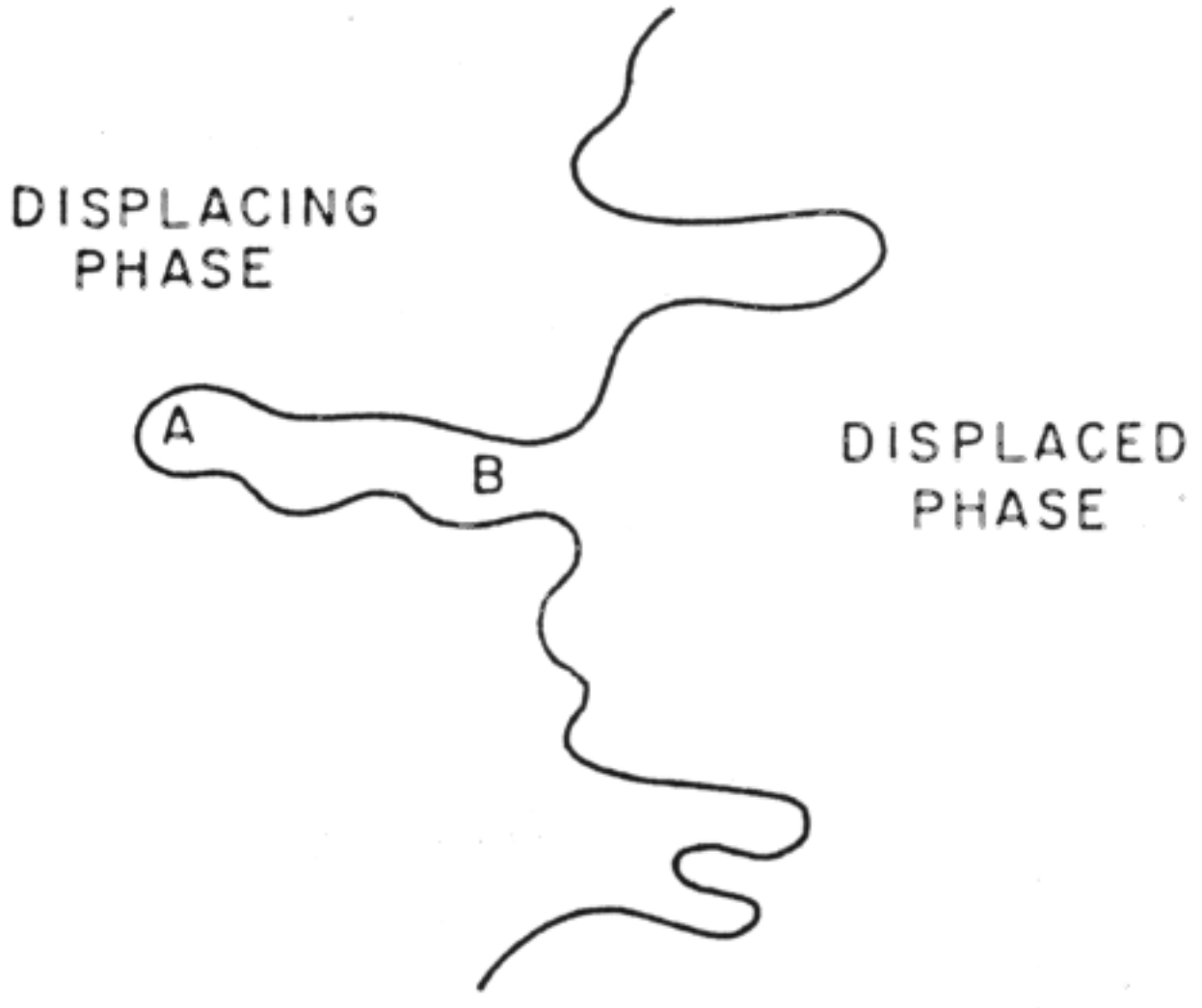

Figure 1: Idealised mechanism for blob entrapment

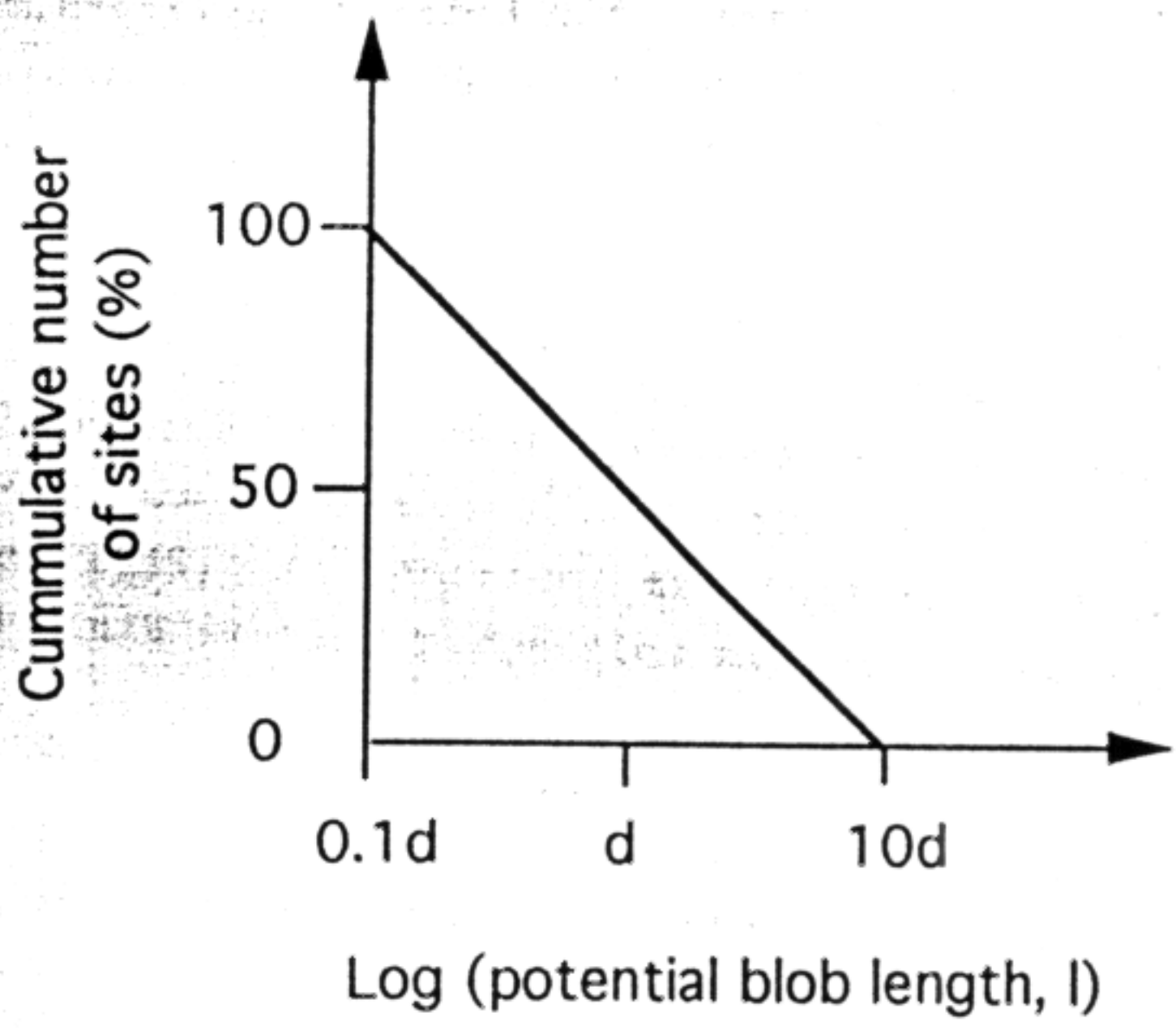

Figure 2: Assumed relationship between the length of a potential blob and the cumulative number of entrapment sites

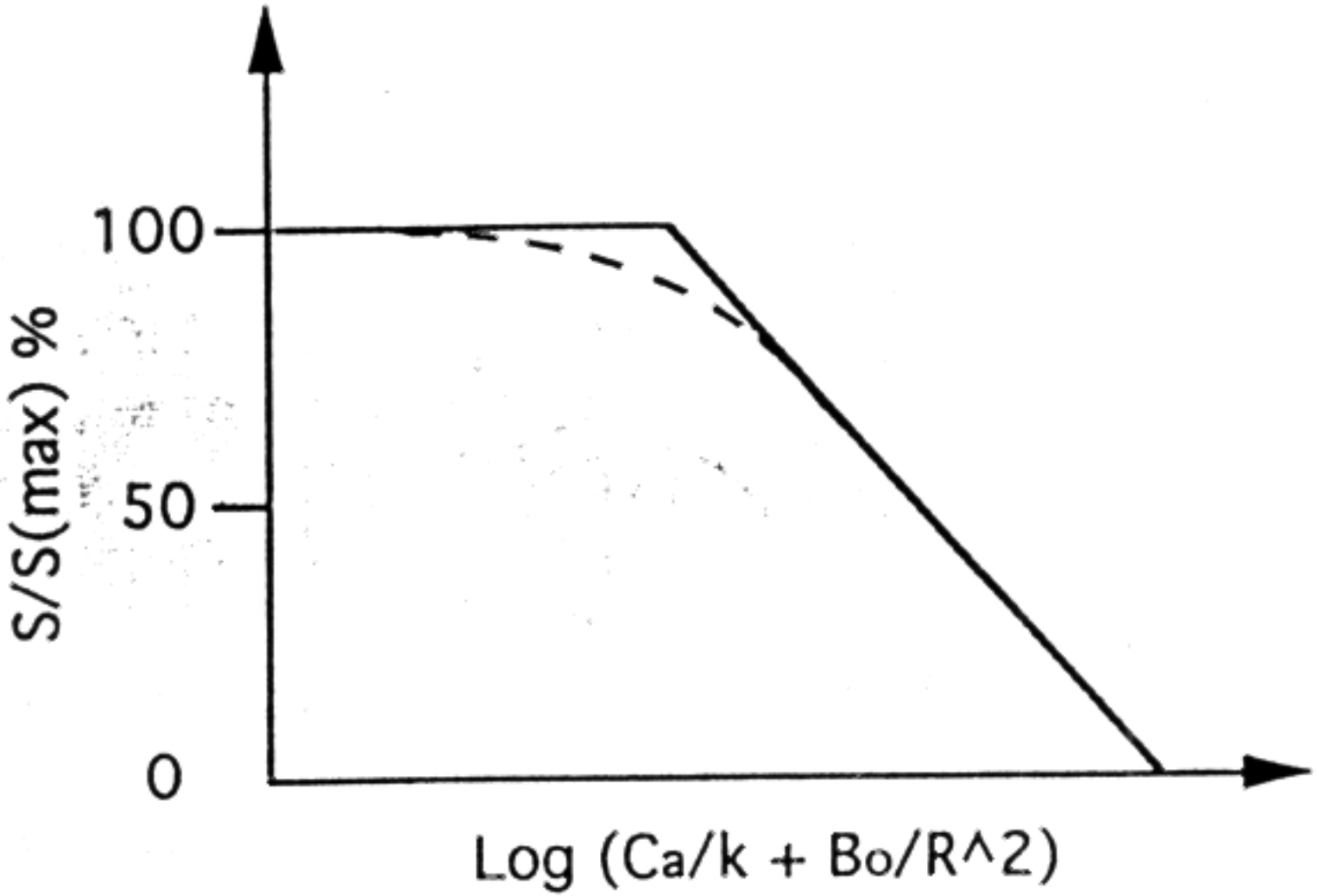

Figure 3: Assumed relationship between entrapped NAPL saturation and C_a and B_o